Technical Paper

ISSN 1997-1400 Int. J. Pavement Res. Technol. 2(3):98-105

Field Structural Performance of Stabilized Blended Calcium Sulfate Materials under Accelerated Pavement Testing

Zhong Wu[1+], Xingwei Chen[1], Louay N. Mohammad[1], and Zhongjie Zhang[1]

Abstract: Blended Calcium Sulfate (BCS), a recycled fluorogypsum mixture, has been used in Louisiana as a pavement base layer for more than a decade. Without further chemical stabilization, the major concern of using raw BCS as a pavement structural layer is its moisture susceptibility. It could cause both short-term construction difficulties and long-term performance problems. In order to verify the efficiency of BCS stabilization schemes that were obtained from laboratory results and further assess the field performance of stabilized BCS materials as well as potential cost benefits, three accelerated pavement test sections including two of different stabilized BCS bases and one of a crushed stone base were recently tested at the Louisiana Pavement Research Facility (PRF) in Port Allen, LA. The three sections shared a common pavement structure. The only difference was the base course materials. Each test section was instrumented with one multi-depth deflectometer and two pressure cells for measuring related pavement responses. Surface distress survey and the falling weight deflectometer (FWD) tests were performed at the end of every 25,000 load repetitions. The overall accelerated loading results indicated that a test section containing the granulated ground blast furnace slag (GGBFS) stabilized BCS base outperformed other two sections by a significantly large margin. FWD backcalculation results indicated that the GGBFS stabilized BCS base generally possessed an in-situ modulus value higher than that for an asphalt concrete layer and performed like a lean concrete. Cost benefit analysis results further indicated that when using the GGBFS stabilized BCS in lieu of a stone base in a flexible pavement design, the asphalt concrete thickness could be considerably reduced thus, the construction costs can be saved immediately.

Key words: *Accelerated pavement testing; Construction cost; Field performance; FWD; Instrumentation; Stabilized base; Stone base.*

Introduction

To design and build a cost-effective pavement structure is a continuous effort for both pavement engineers and researchers. Due to lack of natural resource of high-quality stone aggregates, Louisiana Department of Transportation and Development (LADOTD), still relies on imported aggregates in part of its pavement construction; On the other hand, LADOTD continuously seeks other alternative base materials in lieu of a stone base. One of the alternative base materials is a recycled fluorogypsum, which is an industrial by-product of hydrofluoric acid from fluorspar (a mineral composed of calcium fluoride) and sulfuric acid. For an environmental safety purpose, recycling of fluorogypsum requires adding lime or limestone to raise its pH value. Therefore, a recycled fluorogypsum base course is also called Blended Calcium Sulfate (BCS) base in Louisiana.

Raw BCS base (i.e., without further chemical stabilization) can achieve relatively high strength and stiffness under a dry environment. However, raw BCS material is associated with moisture susceptibility problem. Extra moisture in BCS, which usually exhibits low strength and stiffness due to dilation, can cause both short-term construction difficulties and long-term performance problems.

In a previously completed laboratory study [1], moisture sensitivity and unconfined compressive strength tests were performed on stabilized BCS materials using different chemical stabilizers, such as furnace slag, fly ash, Portland cement, and lime. The results indicated that BCS stabilized with either the grade 120 granulated ground blast furnace slag (GGBFS) or with GGBFS and some secondary stabilizers (Type I Portland cement, lime, or Class C fly ash) could achieve a significantly better performance than the raw BCS in terms of both water resistance and unconfined compressive strength [1,2].

In order to verify the laboratory derived BCS stabilization schemes and further assess the potential economic benefits by field performance, a full-scale accelerated pavement testing experiment was recently conducted at the Louisiana Transportation Research Center's Pavement Research Facility (PRF) in Port Allen, Louisiana.

The objectives of this study were (1) to evaluate the field structural performance of two BCS base materials stabilized with (a) fly ash and (b) GGBFS as compared to a crushed stone base material under accelerated loading, and (2) to assess potential benefits of using stabilized BCS as base course.

Accelerated Pavement Testing (APT)

APT Facility

The APT loading device used was an Australia-designed Accelerated Load Facility (ALF). The ALF device is a 33-*m* long accelerated loading device originally developed in Australia. The ALF wheel assembly models one-half of a single axle with dual tires, and the load is adjustable from 43.4 to 84.4*kN* per load application. With a computer-controlled load trolley, the weight and movement of traffic is simulated repetitively in one direction at a speed of 16.8*km/hr*.

[1] Louisiana Transportation Research Center, Baton Rouge, LA, USA 70808.

[+] Corresponding Author: E-mail zhongwu@ltrc.lsu.edu

Note: Submitted February 16, 2009; Revised April 6, 2009; Accepted April 17, 2009.

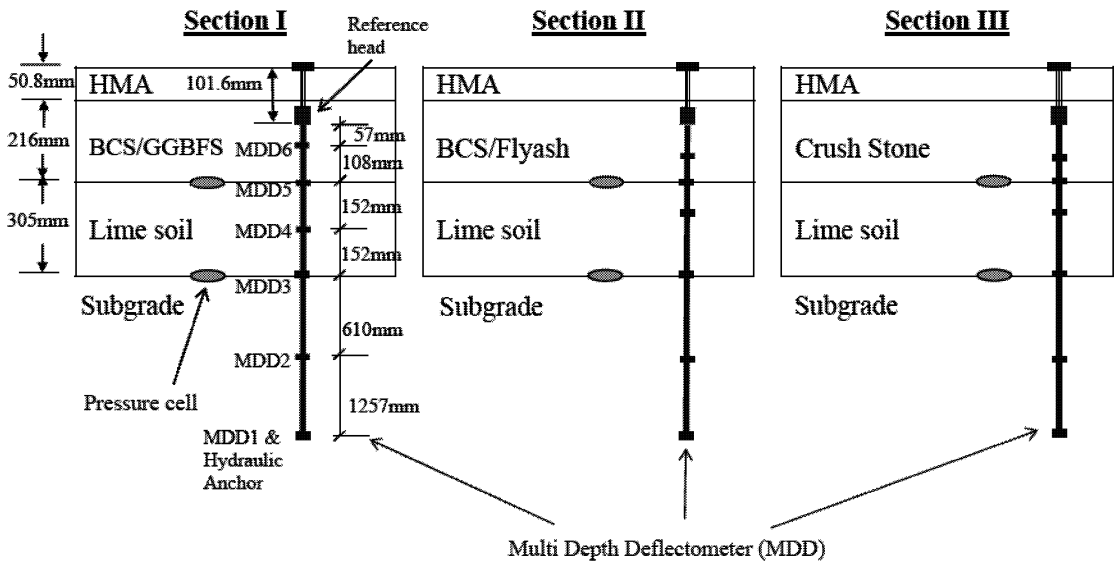

Fig. 1. Pavement Structures of ALF Test Sections.

Table 1. Chemical Composition of Used Stabilizers [1]

Composition (%)	GGBFS	Class C Fly Ash
SiO_2	34.5	47.5
Al_2O_3	9.5	4.1
Fe_2O_3	1.3	5.2
CaO	39.6	20.1
MgO	10.9	2.5
K_2O	1.3	0.7
Na_2O	0.5	0.3

Description of APT Test Sections

Three APT pavement test sections, as outlined in Fig. 1, were constructed using normal highway construction equipments and procedures. Each section was about 4.0*m* wide by 33.0*m* long. As shown in Fig. 1, all three sections had a 50.8*mm* hot mix asphalt (HMA) top layer, a 216*mm* base layer, and a 305*mm* lime-treated subbase layer. A thin HMA layer was used due to the consideration that this APT testing was to investigate the performance of bases layers. Specifically, test Section I had a 10 percent GGBFS stabilized BCS base, Section II used a 15 percent fly ash stabilized BCS base, and section III was the control section, which included a crushed limestone base layer.

The instrumentation used in this experiment included one Multi Depth Deflectometer (MDD) and two pressure cells, which were installed on each test section to measure moving-load induced pavement vertical deformations and vertical stresses. The MDD selected in this study was the SnapMDD manufactured by the Construction Technology Laboratory (CTL). The pressure cells used were the Geokon model 3500 earth pressure cells. More details on instrumentation can be found elsewhere [3].

Materials

A 19*mm* nominal size aggregate Superpave mixture designed at a compaction effort of 100 gyrations was selected in this experiment. This mixture was directly obtained from a construction mix plant nearby, which was also used as the wearing course in a rehabilitation project. The lime soil layer shown in Fig. 1 was a construction "working table" layer mixed in the field using a 10 percent lime by volume and an A-6 soil. The A-6 soil was also used in the subgrade. The subgrade soil was a silty clay, consisting of 60.3 percent silt and 23.5 percent clay with a plasticity index of 10.

The raw BCS material used was supplied by Bear Industries Inc., Port Allen, LA. This material had a pH value of 6.5, and its primary chemical-components included 29 percent CaO and 54 percent SO_4. Two chemical stabilizers, the GGBFS and the Class C fly ash, were supplied by Buzzi Unicem USA of New Orleans and Bear Industries, Inc., respectively. The selected GGBFS material complies with ASTM C989 as a grade of 120. The chemical components of two used stabilizers are listed in Table 1. In general, 10 percent by volume GGBFS and 15 percent by volume Fly Ash were applied into BCS base layers in Sections I and II, respectively, field-mixed, and then compacted to a required construction density. The volumetric moisture content of the GGBFS-stabilized BCS was 29.7 percent, and the volumetric moisture content of the fly ash-stabilized BCS was 43 percent. More details regarding to laboratory and construction results on the stabilized BCS mixtures can be referred to elsewhere [1].

The control base course in Section III was constructed as Class-II stone base courses according to the LADOTD's standard specification for Roads and Bridge [4]. Kentucky crushed limestone was used. The gradation specification requirements for Class-II stone base are listed in Table 2. Note that the optimum dry density for the stone base was 2,390kg/m^3 with an optimum moisture content of 6.3 percent.

Field Monitoring and Failure Criteria

Table 2. Gradation Specification Requirements for Class-II Stone Base [4]

U.S. Sieve	Metric Sieve	Percent Passing
1½ *in.*	37.5 *mm*	100
1 *in.*	25.0 *mm*	90-100
¾ *in.*	19.0 *mm*	70-100
No. 4	4.75 *mm*	35-65
No. 40	425 *μm*	12-32
No. 200	75 *μm*	5-12

Field monitoring of this experiment included the instrumentation data collection at roughly every 8,500 ALF repetitions and the Falling Weight Deflectometer (FWD) tests performed at every 25,000 repetitions. Pavement surface distresses (rutting and cracking), profiles, and HMA temperature were also measured at an interval of 25,000 repetitions.

In this study, a test section was considered to have failed when the pavement condition meets one of the following failure criteria, whichever comes first: (1) the average rut depth reaches up to 12.5*mm* among eight measurement stations within the trafficked area of a section; (2) 50 percent of the trafficked area of a section develops visible cracks (e.g., longitudinal, transverse, and alligator cracks) more than $5m/m^2$.

Loading History

The ALF machine used a dual-tire configuration in this experiment, with two MICHELIN radial 11R22.5 tires inflated to 723*kPa* load. The loading was applied every 25,000 repetitions for three sections in turn until pavement failure. Wander of 190*mm* was adopted in this study. The beginning ALF wheel load was 43.4*kN*. The load magnitude was then raised by adding three more steel plates (each weighs 10.2*kN*) onto the machine in order to accelerate the speeds of failure in the two stabilized BCS test sections. The three steel plates were added each at a time after the ALF load repetitions of 175,000, 225,000, and 325,000, respectively. It should be noted that in the following sections when 80*kN* Equivalent Single Axle Load (ESAL) was used in the discussion, the ESAL numbers were basically translated from the ALF repetitions by using the fourth power law suggested by the 1993 American Association of State Highway and Transportation Officials (AASHTO) Pavement Design Guide [5]. The APT testing lasted one year for Section I, 11 months for Section II, and four months for Section III.

Accelerated Loading Results

FWD Results

Fig. 2 presents the average FWD center deflection (D0) results for the three test sections evaluated. The deflection was first normalized to a 40*kN* load level and then temperature-corrected to 25°C based on a procedure developed under the Long Term Pavement Performance (LTPP) program [6]. A higher center deflection indicates a smaller composite stiffness for a pavement structure. As shown in Fig. 2, the D0 values of Section I were significantly lower than both Sections II and III, whereas Section III had higher D0

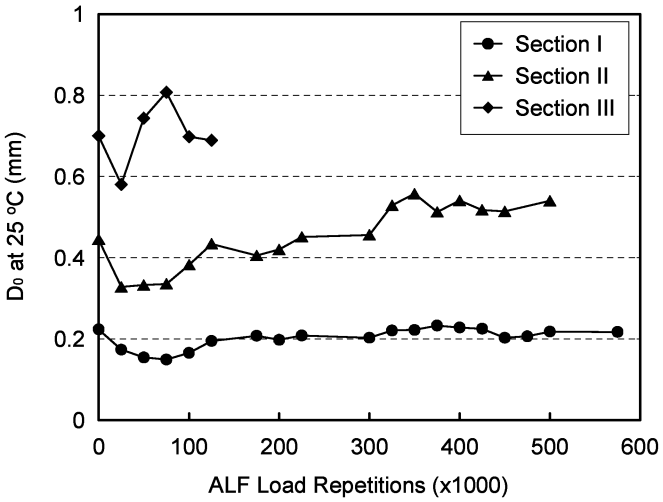

Fig. 2. FWD Center Deflections.

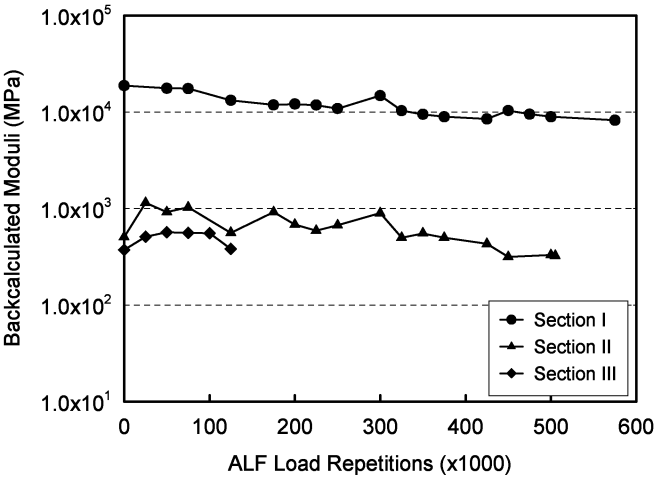

Fig. 3. Backcalculated Moduli of Base Materials.

values than Section II. In addition, an initial decrease in D0 values was presumably due to the post-compaction of pavement layers and the curing of base and subbase materials. Similarly, an increasing trend of D0s indicated the deterioration of pavement materials.

EVERCALC 5.0, developed by Washington Department of Transportation [7], was used in the FWD backcalculation of layer moduli. The initial trials indicated that, if including a very thin HMA layer (50.0*mm*) in the backcalculation, the resulted root mean square (RMS) errors were generally very large. Also, a fairly high modulus value (generally higher than 2,000*MPa*) was found for the lime treated soil layer, which is significantly higher than those obtained in laboratory resilient modulus test on this type of material (a range from 172 to 345*MPa*) [8]. In order to obtain a relatively realistic set(s) of layer modulus for base and other materials, the elastic modulus of HMA layer was set to a fixed value of 5,000*MPa* in all subsequent FWD backcalculations. The RMS errors were generally less than 3 percent for all deflection bowls evaluated. Fig. 3 presents the backcalculation results for the three base materials considered. As can be seen in the figure, all three materials showed a decreasing trend in stiffness as the ALF load repetitions increased, presumably due to material deterioration under trafficking. The BCS/GGBFS base had a significantly higher in-situ modulus (>10

Table 3. Results of the Measured Vertical Compressive Stresses.

Section	Statistics	Vertical Stress (*kPa*)	
		At Bottom of Base	At Bottom of Subbase
I	Avg	6.2	3.5
	Std	0.7	0.7
	COV	11%	20%
II	Avg	35.8	12.4
	Std	3.5	1.4
	COV	10%	11%
III	Avg	234.5	4.1
	Std	59.3	1.4
	COV	25%	34%

times) than both BCS/Fly ash and crushed stone, while the modulus of BCS/Fly ash was about two times greater than that of the stone. The FWD backcalculation results indicated that in-situ modulus of a BCS/GGBFS layer could be achieved higher than the modulus of a HMA layer.

Instrumentation Results

Table 3 presents a statistical summary of measured vertical compressive stresses obtained from two pressure cells installed on each test section. Only the pressures measured under a 43.4*kN* ALF moving load were listed in Table 3. This was because Section III was failed under this load, and the responses of the three test sections need to be directly compared.

As shown in Table 3, under a dual tire load of 43.4*kN*, the average vertical compressive stresses at the bottom of base layers were respectively 6.2, 35.8, and 234.5*kPa* for Sections I, II, and III, whereas those values on top of a subgrade were 3.5, 12.4 and 4.1*kPa*, respectively. Such results indicate that the stiff BCS/GGBFS material in Section I showed a significantly larger load spreading angle than the other two base materials. In addition, the BCS/Fly ash base in section II also distributed the load better than the stone base in Section III. As stated earlier, data was collected roughly at every 8,500 load repetitions. The coefficient of variation (COV) shown in Table 3 may be related to the variation of pavement responses (vertical compressive stresses) due to the combination effects of seasonal variations (e.g., temperature and moisture) and pavement material deterioration under trafficking. In general, the highest COV value was found for the measurement on top of the subgrade layer in Section III (the stone base section).

The measured vertical compressive stresses were further compared to those analytical values estimated from a multi-layer elastic analysis program, ELSYM5. Backcalculated moduli obtained from an initial FWD test were used in the analysis. Table 4 presents the measured and calculated vertical compressive stresses on the three lanes tested.

As shown in Table 4, stress ratios between the calculated and the measured were generally ranged from 0.4 to 5.5 with the highest and lowest ratios falling in the stone test section (Section III). The discrepancy between the predicted and the measured values is certainly due to the limitations of using the multi-layer elastic theory.

Table 4. Comparison of Measured and Calculated Vertical Compressive Stresses.

Section	Vertical Stress @ bottom of Base (*kPa*)		Cal./Meas.	Vertical Stress @ bottom of Subbase (*kPa*)		Cal./Meas.
	Measured	Calculated		Measured	Calculated	
Section I	6.2	24.2	3.8	3.5	12.4	3.5
Section II	35.8	75.2	2.1	12.4	23.5	1.9
Section III	234.5	95.2	0.4	4.1	22.8	5.5

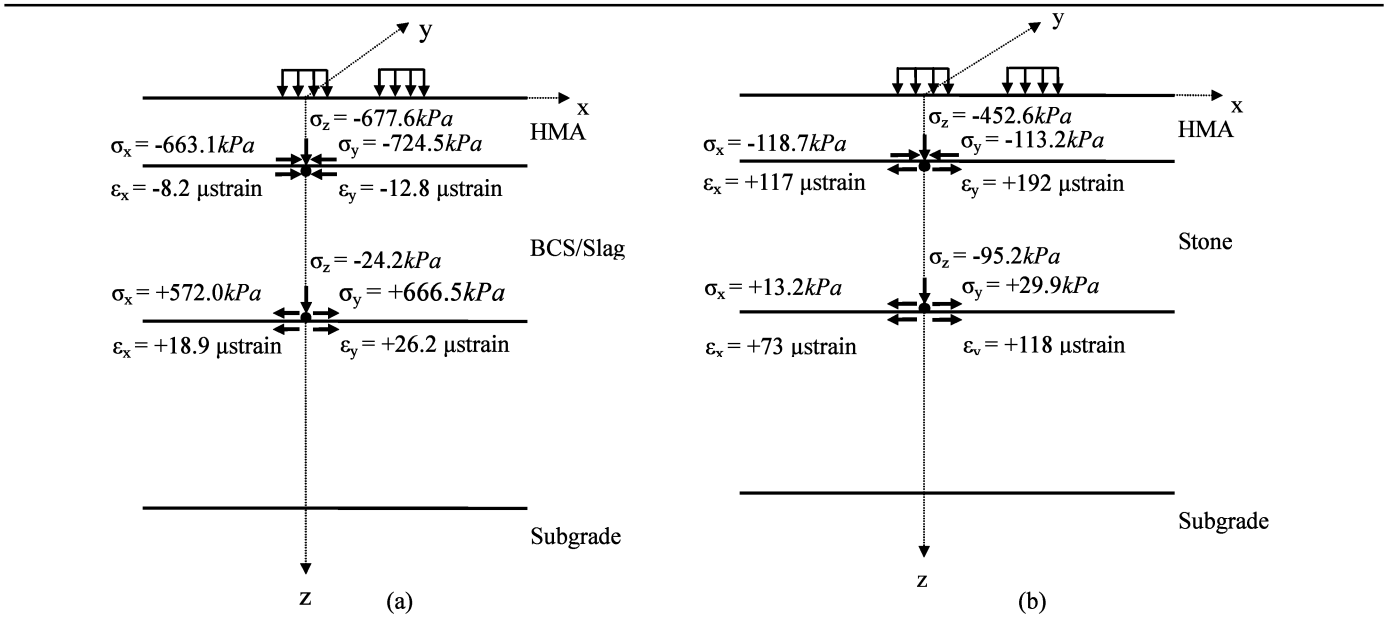

Fig. 4. Stress and Strain Predictions in (a) Section I and (b) Section III. ("+" tension and "-" compression)

However, it is interesting to notice that in Table 4 only the calculated vertical stress at bottom of the stone base in Section III was found smaller than the measured one, whereas in all other cases, the predicted values were higher. Previous studies [9, 10] did show that, on the basis of the elastic layer theory, the calculated vertical stress at bottom of unbound aggregate bases is generally half of the measured value. This seems to match well with the results obtained from the stone base in this study. However, the question is: why does the elastic layer theory only overpredict vertical stress values for a stone base? The answer for this question may be illustrated by analyzing the predicted stress and strain distribution using the elastic layer theory.

Fig. 4 presents the predicted stresses and strains at top and bottom of both base layers in sections I and III. As shown in Fig. 4(a), a tension zone (based on the predicted tensile strains) goes from somewhere inside the BCS/GGBFS base layer of Section I. However, Fig. 4(b) shows that the same tension zone in Section III will start from the middle of the HMA layer and then go all the way to the bottom layers. This indicates that the entire stone base layer is predicted under a tension zone in which large tensile strains are developed in both x-y directions (*see* σ_x and σ_y in Fig. 4(b)). In reality, a stone layer can not resist any significant tension because the material is unbound. If a stone aggregate layer received a large tension, the stone particles would begin to separate from each other. Therefore, the possible segregation of stone particles due to tension may explain why higher than theory predicted vertical stresses could be measured from an unbound base layer, such as the stone layer in Section III.

On the other hand, as shown in Fig. 4(a), only the bottom part of the BCS/GGBFS layer is predicted under a small tension. Such tension would not easily cause a particle separation because the BCS/GGBFS is a bound material, which can endure somewhat tensile strains. Besides the limitation of a multi-layer elastic theory, the discrepancy between the predicted and the measured vertical compressive stresses in BCS/GGBFS and other bounded layers may be partially attributed to the limitations of the pressure cell used. As pointed out by Dunnicliff [11], if the pressure cell stiffness is less stiff than soil stiffness, then the cell tends to under-register, which will result in a smaller pressure value. In fact, the stiff BCS/GGBFS layer in Section I seems to be an extreme example for this phenomenon. As its modulus is significantly higher than any other base layers, the predicted vertical stress was found about three times higher than the measured value, as seen in Table 4.

MDD Results

The plastic deformation measured from MDD was used to determine the permanent deformation developed at each pavement structural layer. Note that the MDDs installed on this experiment were considered partially successful. All three MDDs functioned properly in the beginning of loading. However, the MDDs installed on Sections I and II only lasted for about 225,000 and 340,000 load passes, respectively, before the MDD baselines started to move. MDD installed on Section III was survived until this section was failed. However, the number of load repetitions on Section III was only 125,000 ALF passes. Discussion on why the MDDs failed is beyond the scope of this paper [12].

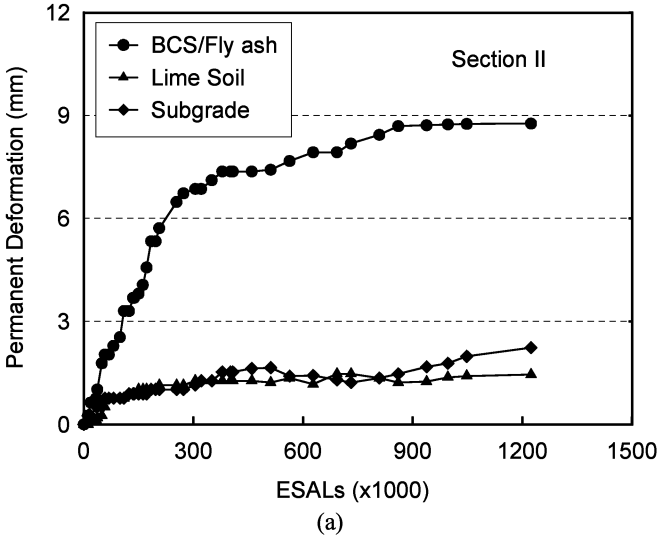

(a)

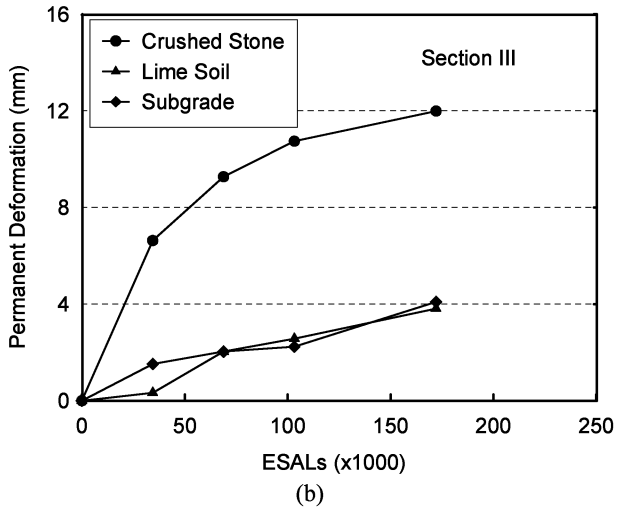

(b)

Fig. 5. Permanent Deformations in Each Layer at Section (a) II and (b) III by MDD.

Fig. 5 presents the MDD measured permanent deformation results for Sections II and III. Section I's MDD results were not reported here because only a very small permanent deformation (less than 2*mm*) was observed on this section during the first 225,000 repetitions before the MDD was failed. Therefore, such negligible amount of permanent deformation is not appropriate to be further distributed to different pavement layers. Generally, noticeable amounts of permanent deformations were observed on both Sections II and III.

Fig. 5(a) indicates that a significant amount of permanent deformation was developed on the BCS/Fly ash layer with a similar small amount of permanent deformation developed on both the lime-treated soil and the subgrade. As shown in Fig. 5(b), a large amount of permanent deformation was also observed on the base layer (crushed stone). The MDD results indicated that the stone layer, lime-soil layer, and subgrade each contributed 70, 15, and 15 percent, respectively, to the total surface rut depth developed in the MDD station. In general, the MDD plastic deformation results appeared to agree well with the vertical compressive stress results described above. The base layers of both Sections II and III developed

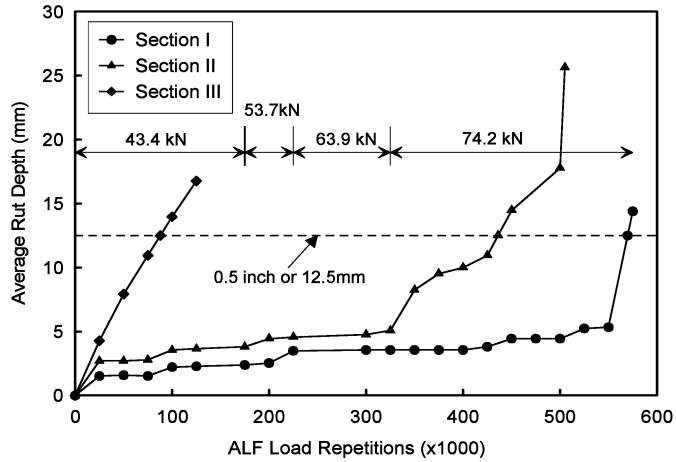

Fig. 6. Rut Depth Developments on Test Sections.

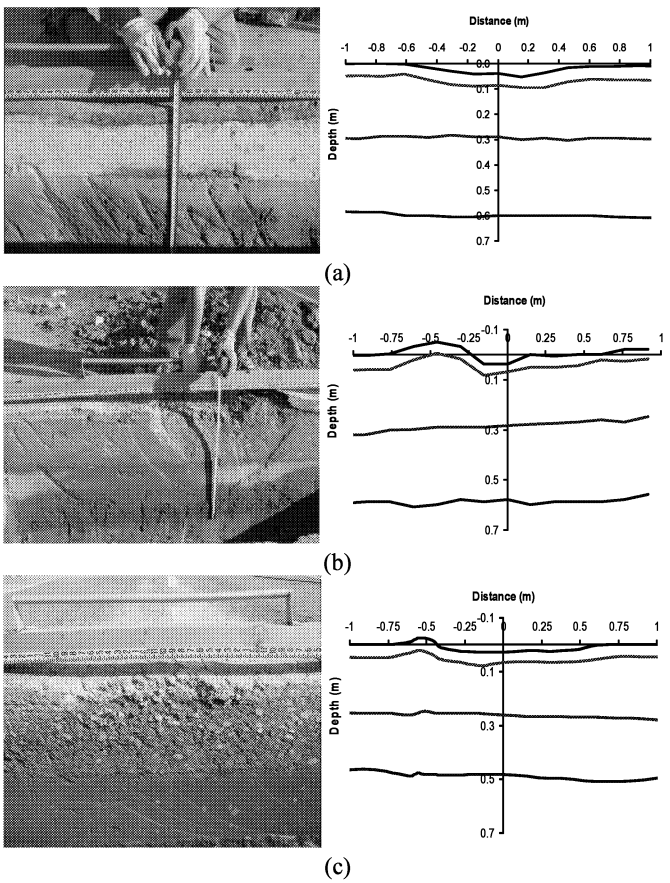

Fig. 7 Post-Mortem Trench Results in Section (a) I, (b) II, and (c) III.

large permanent deformation due to receiving higher vertical stress than the bottom layers. However, to achieve a similar permanent deformation, Section II with a fly ash stabilized BCS base required a significantly larger number of load repetitions than section III with a stone base, as shown in Fig. 5. The MDD measured permanent deformation is very useful in better understanding of material behavior in a pavement structure. It also can be used in calibrate rutting model, such as the one used in the newly developed M-E Pavement Design Guide. Additional research using those MDD measurements is under investigation.

Measured Surface Rut Depths

Fig. 6 provides the average rut depth development for the three sections tested measured by an "A-Frame" apparatus. The corresponding ALF load levels at different load repetitions are also provided in the figure. According to the failure criteria, all three sections were considered as rutting failure. No visible fatigue or alligator cracks were observed on Section I or II when the average rut depth reached to the 12.5*mm* limit. On the other hand, Section III developed some medium-severe alligator cracks at its rutting failure point

As shown in Fig. 6, Section I with a BCS/Slag base performed significantly better than the other two sections by receiving a total number of 570,000 ALF repetitions before its reaching of the 12.5*mm* rutting limit. Next was Section II with a BCS/Fly ash base and 436,000 total repetitions at a rutting failure. The last performed section was Section III, whose base was a crushed stone and only lasted 86,000 passes before reaching a failure.

Post-Mortem Trenches

Fig. 7 shows transverse trench results for the three test sections investigated. Each trench was about 0.6*m* wide and 3.0*m* long. The measured transverse profiles in Fig. 7 indicate that both Sections II and III had a base shear flow failure, whereas Section I failed primarily due to further densification of the BCS/GGBFS base layer under the load. No visible deformation was observed on the trench below the BCS/GGBFS layer. The shear failures in Sections II and III could be attributed to the very thin HMA layer used. However, it also indicated insufficient shear strengths for those base materials. The shear flow failure in Section II raised a concern for the BCS/Fly ash material because in previous laboratory tests this material still possessed significant moisture susceptibility [1]. Even though Section II performed considerably better than Section III, the long term performance of the BCS/Fly ash as a base material under a wet environment still could not be drawn from this APT experiment.

Construction Cost Analysis

The APT results indicated that the GGBFS stabilized BCS base in Section I outperformed two other base materials (BCS/Fly ash and stone) by a significantly large margin. The field evidence for supporting this indication include the smallest FWD center deflections, negligible permanent deformation at the first 225,000 ALF passes, smallest vertical compressive stresses at two depths, no visible surface cracking and a longest pavement rutting life. Post-mortem trench results further revealed that, even at the end of a rutting failure, the GGBFS stabilized BCS base in Section I was observed to hold well together as a lean concrete layer. In addition, the fly ash stabilized BCS base was also found to perform better than the stone base evaluated. However, due to its potential water susceptibility, the long term performance of using a fly ash stabilized BCS as a base material under a wet environment is still questionable. Therefore, in lieu of the crushed stone base, it is concluded that the 10 percent GGBFS stabilized BCS should be a very good candidate based on its outstanding structural performance.

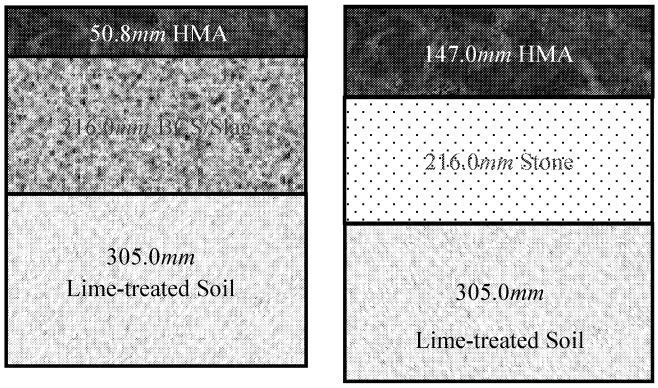

Fig. 8. Pavement Alternatives Used in Cost-Benefit Analysis.

Table 5. Initial Construction Costs.

Alternative A Materials	Unit Prices ($)	Quantity	Construction Costs($)
50.8*mm* HMA	92.4 per ton	838.9 ton	77,514.36
216*mm* BCS/GGBFS	37.2 per m^2	6,376.1m^2	237,190.92
305*mm* Lime-Treated Soil	23.1 per m^2	6,376.1m^2	147,287.91
Total Initial Construction Costs			$461,993.19

Alternative B Materials	Unit Prices ($)	Quantity	Construction Costs($)
147*mm* HMA	92.4 per ton	2432.9 ton	224,799.96
216*mm* Stone	27.6 per m^2	6,376.1m^2	175,980.36
305*mm* Lime-Treated Soil	23.1 per m^2	6,376.1m^2	147,287.91
Total Initial Construction Costs			$548,068.23

On the other hand, whether the BCS/GGBFS material should be used in a pavement design also depends on its economic aspect. To demonstrate cost benefits from using GGBFS stabilized BCS materials, a construction cost analysis was performed on two pavement structure alternatives. As outlined in Fig. 8, Alternative A had a same pavement structure as Section I, whereas, Alternative B used a similar structure as Section III with different HMA thickness. The two alternatives were designed to have a same design structural number (SN). According to the 1993 AASHTO Design Guide, both alternatives should be expected to have a same future performance and pavement lives. The SN value was determined based on layer thicknesses and layer coefficient values *(5)*. A layer coefficient of 0.34 was assigned for a BCS/GGBFS base layer, which was determined from the APT performance results [12]. The layer coefficients of new HMA and crushed stone layers were assumed to be 0.44 and 0.14, respectively. No structural value was assigned to a lime-treated "working table" layer based on engineering judgment. By using those layer coefficients and thickness values shown in Fig. 8, both alternative pavement structures would result in a total SN value of 3.77. Such design results indicated that by using a GGBFS stabilized BCS base in lieu of stone, the thickness of the HMA layer could be significantly reduced (i.e., a 97.0*mm* reduction as comparing Alternative A and B, as shown in Fig. 8).

The construction costs of two pavement alternatives are listed in Table 5. The unit prices in the table were determined from the construction costs of this APT experiment. The quantities were calculated based on a 3.96*m* wide lane for one mile long. As shown in Table 5, the estimated construction costs for Alternatives A and B were $461,993.19 and $548,068.23, respectively. Therefore, by using a GGBFS stabilized BCS base in lieu of a stone base, the estimated cost benefits would be $86,075 per lane mile. Applying the estimated cost benefits to a typical 2-lane, 16-*km* long roadway rehabilitation project, the use of a GGBFS stabilized BCS base in lieu of a stone base can result in a total construction cost savings up to $1,725,440.

Summary and Conclusions

The APT experiment of this study was designed to evaluate the performance of two chemically stabilized BCS base materials as compared to a crushed stone base. Three APT test sections, each differed only in a base material, were tested under the Louisiana ALF. Each test section was instrumented with one MDD and two pressure cells for measuring related pavement responses under an ALF wheel load. Surface distress survey and FWD deflection tests were performed regularly at the end of each 25,000 load repetitions. The overall APT results indicated that a 10 percent GGBFS stabilized BCS base material outperformed two other base materials (i.e., a 15 percent fly ash stabilized BCS and a Class-II stone) by a significantly large margin. In terms of overall structural performance and rut-resistance, the GGBFS stabilized BCS base material was found significantly better than a Class-II stone base. Therefore, depending on the material availability and economic consideration, the GGBFS stabilized BCS base material is highly recommended to be used in lieu of a stone base when needed.

Some specific observations and conclusions can also be drawn from this study:

- The FWD backcalculation results indicated that in-situ modulus of a BCS/GGBFS layer could be achieved higher than the modulus of a HMA layer, which resulted in a flexible pavement structure with a stronger base layer underneath a surface HMA layer.
- It is known that the discrepancy between predicted and measured pavement responses is mainly due to the limitations of using the multi-layer elastic theory. However, it was found that the multi-layer elastic theory seemed only to over-predict the vertical compressive stresses developed in an unbound aggregate layer but under-estimate the stresses for other bounded base materials used in this study. This was because the elastic theory tends to predict a large tension zone inside a base layer, which is not realistic for an unbound material to endure under a real pavement condition. On the other hand, stiff materials, e.g., BCS/GGBFS, can cause a pressure cell to under-register, and in return, the pressure cell provides a smaller pressure value.
- MDD results indicated that most of the permanent deformation was from the base layers evaluated. Using the MDD to measure permanent deformation is very useful in better understanding the material behavior in a pavement structure. It also can be used in calibrate rutting model, such as the one used in the

newly developed M-E Pavement Design Guide. Additional research of using those MDD measurements is under investigation.

- A 15 percent fly ash stabilized BCS base was also found to perform better than the stone base evaluated. However, post-mortem trench results revealed that this material was failed due to a large shear flow. Because there was still a concern regarding its water susceptibility, the long term performance of using a fly ash stabilized BCS as a base material under a wet environment could not be determined from this experiment.
- A construction cost analysis demonstrated that, by using a GGBFS stabilized BCS base in lieu of a stone base, the thickness of a HMA layer could be significantly reduced. Therefore, the initial construction cost of using a GGBFS stabilized BCS base in a pavement structure will be considerably cheaper than a pavement with a thicker HMA layer and a stone base.

References

1. Zhang, Z. and Tao, M., (2006). Stability of Calcium Sulfate Base Course in a Wet Environment, *LTRC Report No. 419*, Baton Rouge, LA, USA.
2. Tao, M. and Zhang, Z., (2005). Enhanced Performance of Stabilized By-Product Gypsum, *Journal of Materials in Civil Engineering*, 17(6), pp. 617-623.
3. Wu, Z., Zhang, Z., King, B., Raghavendra, A., and Martinez, M., (2006). Instrumentation and Accelerated Testing on Louisiana Flexible Pavements, *Airfield and Highway Pavements – Meeting Today's Challenges with Emerging technologies*, ASCE Special Publication, Edited by I. L. AL-Qadi, pp. 119-130.
4. Department of Transportation and Development, (2000). *Louisiana Standard Specifications for Roads and Bridges*, State of Louisiana, Baton Rouge, 2000 Edition.
5. American Association of State Highway and Transportation Officials (AASHTO), (1993). *AASHTO Guide for Design of Pavement Structures*, Washington, DC, USA.
6. Lukanen, E.O., Stubstad, R., and Briggs, R., (2000). Temperature Predictions and Adjustment Factors for Asphalt Pavement, *Publication NO. FHWA-RD-98-085*, Federal Highway Administration, McLean, VA, USA.
7. Pierce, L.M. and Mahoney, J.P., (1996). Asphalt Concrete Overlay Design Case Studies, *Transportation Research Records*, No. 1543, pp. 3-9.
8. Mohammad, L., Herath, A., Rasoulian, M., and Zhang, Z., (2006). Laboratory Evaluation of Untreated and Treated Pavement Base Materials from a Repeated Load Permanent Deformation Test, *the 85th Transportation Research Board Annual Meeting,* Transportation Research Board of the National Academies, Washington, DC, USA, CD-ROM.
9. Ullidtz, P., Askegaard, V., and Sjolin, F.O., (1996). Normal Stresses in a Granular Material Under Falling Weight Deflectometer Loading, *Transportation Research Records*, No. 1540, pp. 24-28.
10. Ullidtz, P., (2007). Deterioration Models for Managing Flexible Pavements, *Transportation Research Records*, No. 1655, pp. 31-34.
11. Dunnicliff, J., (1993). *Geotechnical Instrumentation for Monitoring Field Performance*, Wiley, New York.
12. Wu, Z., Zhang, Z., and Morvant, M., (2008). Performance of Various Base/Subbase Materials under Accelerated Loading, *the 87th Transportation Research Board Annual Meeting,* Transportation Research Board of the National Academies, Washington, DC, USA, CD-ROM.